Formation and annihilation of a bond defect in silicon: An *ab initio* quantum-mechanical characterization

F. Cargnoni and C. Gatti
Centro CNR per lo Studio delle Relazioni fra Struttura e Reattività Chimica, via Golgi 19, I-20133 Milano, Italy

L. Colombo
Istituto Nazionale per la Fisica della Materia and Dipartimento di Scienza dei Materiali, Università degli Studi di Milano, via Emanueli 15, I-20126 Milano, Italy

(Received 12 June 1997)

The electronic structure and bond properties of a lattice defect in silicon formed by the incomplete recombination of a vacancy-interstitial pair are described by combining tight-binding molecular-dynamics and *ab initio* Hartree-Fock calculations. The defect structure consists of a large nuclear distortion nearly perfectly compensated by electron charge rearrangment. The reaction path for its annihilation is reported and described in terms of an electron-density topological analysis within the quantum theory of atoms in molecules approach. [S0163-1829(98)04001-6]

I. INTRODUCTION

The migration and interaction of native point defects in silicon affects many micro- and mesoscopic properties of bulk samples (e.g., mass transport, annealing of implantation damage, crystal-to-amorphous transition, nucleation of extended defects). The physics of the vacancy and self-interstitial has attracted, therefore, several theoretical and experimental studies aimed to derive an accurate atomic-scale model of their formation, migration, and interaction.

Coalescence of like defects determines intermediate steps for the formation of microdefects, like voids or dislocation loops. On the other hand, the interaction between defects of different species governs the microstructural evolution far from equilibrium, e.g., during ion implantation. As for the latter process, it has been recently demonstrated[1] that a barrier for the annihilation of a vacancy-interstitial pair exists. This result was obtained by means of tight-binding molecular dynamics (TBMD) computer simulations and confirmed previous suggestions[2] based on experimental evidence. In Ref. 1, Tang *et al.* showed that whenever a single vacancy (V) and self-interstitial (I) approach each other from distances larger than two bond lengths, a defect, named the *I-V complex*, is created. The structure is not a number defect, since it does not involve any deficit or excess of atoms. Rather, it consists in a large and locally confined geometrical deformation of the crystal lattice as due to the rotation of a Si–Si bond in the $\langle 110 \rangle$ plane (i.e., in the plane containing the self-interstitial defect which corresponds to the $\langle 110 \rangle$ dumbbell).

The *I-V* complex is rather stable at room temperature, the energy barrier for its recombination being ~ 1.2 eV, according to TBMD simulations. The resulting lifetime of the defect ranges from the order of hours at $T = 300$ K to microseconds at high temperatures (typical of an annealing process). Moreover, the annihilation path of the *I-V* complex requires a sizeable perturbation in the bond pattern of the host matrix. Therefore, such a defect could play some role in the microstructural evolution of silicon in various conditions such as, for instance, under irradiation.

In this work we present a comprehensive theoretical investigation of the chemical nature and bonding properties of the *I-V* complex. Our goal is to provide a complete and accurate atomic-scale description of the ground-state electronic structure of the defect, as well as to characterize the annihilation reaction which recovers the usual diamond lattice. To this aim we combine TBMD simulations—used to generate the defect structure—with *ab initio* Hartree-Fock calculations and the analysis of the resulting wave functions in order to solve and enlighten the electronic structure properties. The theoretical methods used in this work are described in Sec. II, while the results of our investigation are presented and discussed in Sec. III.

II. COMPUTATIONAL DETAILS

A. The defect geometry

In Fig. 1 we show the atomic equilibrium configuration of the *I-V* defect. This structure was obtained by placing a vacancy at the third nearest-neighbor position of a self-interstital dumbbell along the $\langle 110 \rangle$ direction (i.e., in the plane containing the dumbbell). After that, atomic relaxation was allowed by TBMD. A 216-atom simulation cell and the tight-binding representation by Kwon *et al.*[3] were used. Further details about the defect generation can be found in Ref. 1, whereas a preliminary investigation of the electronic structure of the *I-V* complex is reported in Ref. 4.

The TBMD simulation predicts the two defective atoms to be substantially tetracoordinated, with an internuclear distance shorter (2.27 Å) than in the ideal lattice (2.36 Å), one regular silicon atom lying at 2.46 Å and the remaining two at 2.39 Å. The analysis of the electronic structure of the *I-V* complex confirms the tetracoordination of the defective atoms and the covalent bulklike nature of their bonding interactions.

It is apparent from Fig. 1 that the defect has actually no reminiscence of its origin, namely an interstitial-vacancy

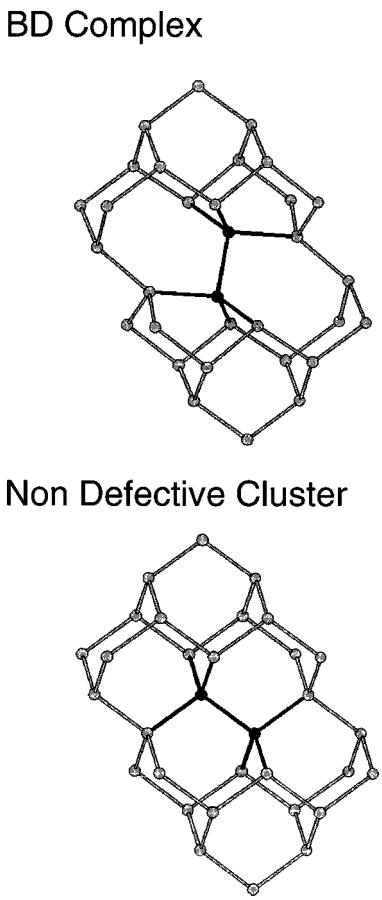

FIG. 1. Stick-and-ball representation of the equilibrium geometry of the BD complex (black circles).

pair. In other words, the structure is better described as a *bond defect* (BD) rather than a two-defect complex. Hereafter we will refer to the *I-V* complex as the *BD complex*. The electron density analysis reported in the following will substantiate this statement.

As for the BD annihilation, five representative silicon cluster structures (set I) were selected for our electron density investigation from the 216-atom TBMD simulation.[1] Each cluster was built by expanding a centersymmetric cluster of 32 Si atoms around the midpoint of the internuclear axis of the BD complex and by saturating the resulting dangling bonds with 38 pseudohydrogen atoms,[5] placed at the corresponding Si atom positions of the TBMD simulation. As evidenced in Fig. 1, no double-bonded hydrogens were introduced in any of the considered clusters.[4] Figure 2 shows the structural arrangement of Si atoms around the BD complex, along its evolution. The angle $BA'A$ changes from 43° in the BD defect (top panel) to the tetrahedral value in the nondefective cluster (bottom panel). Variations of this angle along the BD evolution sketch a reaction path coordinate s ($s=0$, BD complex; $s=1$, nondefective cluster).

In order to study the effect of the constraint of constant AA' distance during the TBMD simulation,[1] a second set (set II) of smaller clusters was built, each one consisting of the eight innermost Si atoms caged by 18 H atoms placed at Si-H $=1.48$ Å. The set II cluster geometries were then optimized by freezing only the H atom locations and the reaction coordinate s.

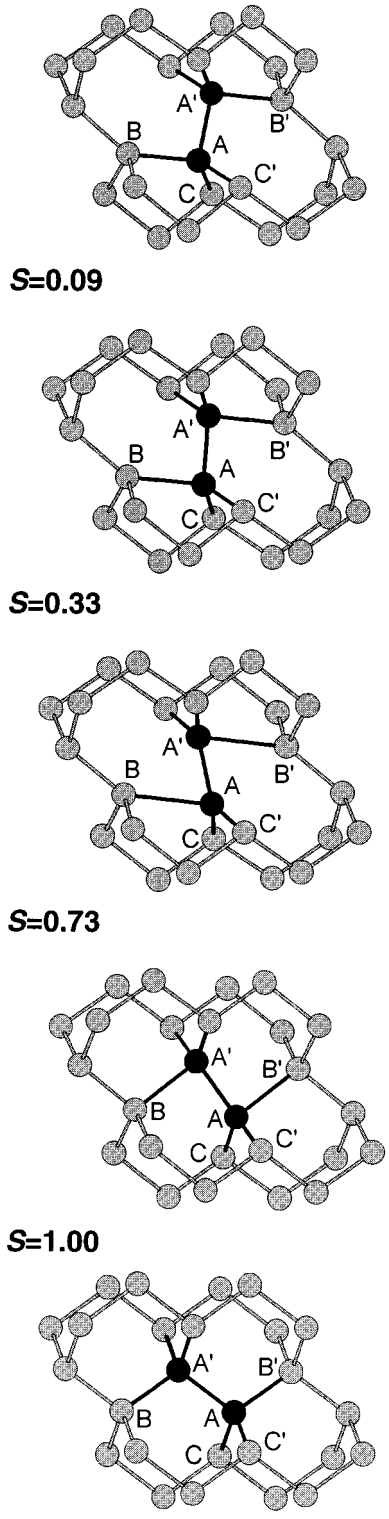

FIG. 2. Stick-and-ball representation of the BD complex along the reaction path s for its annihilation. $s=0$: BD complex; $s=1$: nondefective crystal. The connectivity of Si atoms is inferred from the electron density analysis.

B. Methods

The wave functions for the investigated systems were evaluated with the *ab initio* restricted Hartree-Fock (RHF) method, using a finite basis set of Gaussian functions, in the

usual molecular orbital as a linear combination of atomic orbital approximation.[6] By using only restricted spin orbitals (RHF formalism) we assume that no radical intermediates are involved in the BD rearrangement.[7] Although the RHF method is of a less standard use than density-functional approach in solid-state physics, the former has recently achieved considerable success in the description of crystalline systems. In particular Pisani *et al.*[8] have shown that periodic RHF calculations on crystalline silicon (using a double-Z-plus polarization basis set) are able to reproduce the electron density and the electron moment distribution almost within the experimental error. This result is in agreement with the second-order errors for all one-electron operators guaranteed by the exact HF solution.[9] Furthermore, the use of a local (Gaussian)—as opposed to nonlocal (e.g., plane wave)—basis set is mandatory in our case owing to the local character of the BD complex and of its annihilation process.

The electron density rearrangement along s was investigated within the quantum theory of atoms in molecules (QTAM) approach. A comprehensive exposition of QTAM is given in Ref. 10, while a very condensed outline on the physical basis of this theory may be found in a recent issue of this journal.[11] Applications of QTAM to solid-state packing effects on electron density[12] and to the description of structural changes in solids[13,14] have recently appeared. Central to the QTAM theory is the definition of proper open systems, that is of that subset of the open subsystems of any system which are described by correct equations of motion for their observables. These subsystems are identified within QTAM with the *atoms in a molecule* or, more generally, with the atoms in any assembly of atoms like a cluster or a crystal. The definition of an atom in a molecule Ω, of the average values of its observables and of their equations of motion are obtained through a generalization of the variation of the action-integral operator introduced by Schwinger[15] in the derivation of the principle of stationary action. This generalization is unique as it applies only to regions of real space that satisfy a particular constraint on the variation of the action integral of the subsystem Ω, a constraint that requires Ω to be bounded by a surface S of local zero flux in the gradient vector of the electron density $\rho(\mathbf{r})$

$$\nabla\rho(\mathbf{r})\cdot\mathbf{n}(\mathbf{r})=0 \quad \forall\mathbf{r}\in S\,. \tag{1}$$

Since the electron distribution for a many-electron system generally exhibits local maxima only at the positions of nuclei, the quantum boundary condition given in Eq. (1) yields a partitioning of a chemical system in a disjoint set of mononuclear regions or atoms. As a result of this partitioning the system average of an observable is given by a sum of atomic contributions. In this paper we will detail the changes along s of the atomic electron populations $N(\Omega)$

$$N(\Omega)=\int_{\Omega}\rho(\mathbf{r})d\tau \tag{2}$$

and of the atomic first moments $\mu(\Omega)$

$$\mu(\Omega)=-\int_{\Omega}(\mathbf{r}-\mathbf{r}_{\Omega})\rho(\mathbf{r})d\tau, \tag{3}$$

where $\mathbf{r}_{\Omega}$ denotes the position of the nucleus of the corresponding atom. Atomic moments account for the polarization of the atomic electron densities, due to chemical bonding and chemical bonding distortions. Atomic changes along s are also enlightened by variations in the atomic volumes $V(\Omega)=\int_{\Omega}d\tau$, where—in order to get a finite value—the integration is over the region of space Ω enclosed by the intersection of the atomic surface of zero flux with a particular envelope of the electron density.[16] The $V002(\Omega)$ values used in this paper correspond to the 0.002 a.u. envelope. These volumes yield molecular sizes that can be employed in describing the closer packing found in the solid state.[17] The QTAM permits the investigation of chemical systems on a common basis, as the theory uses only information contained in the electron density $\rho(\mathbf{r})$. No arbitrary partitioning of the molecular electron density in the Hilbert space spanned by the adopted basis set is introduced as it is common in Mulliken's population analysis[18] or one of its many modifications.

In addition to determining the boundary condition for a proper open system, the gradient vector field of $\rho(\mathbf{r})$ also provides a definition of the molecular structure or generally of the pairwise interactions present in an assembly of atoms. Two atoms Ω and Ω' are linked to one another if their nuclei are connected by a line, the atomic interaction line (AIL), where $\rho(\mathbf{r})$ is a maximum with respect to any lateral displacement from the line. The point $\mathbf{r}_c$ where the density attains its minimum value along an AIL is a critical point in $\rho(\mathbf{r})$ [i.e., $\nabla\rho(\mathbf{r}_c)=0$] and it is called a bond critical point (BCP). Each $\Omega-\Omega'$ pairwise interaction has associated its corresponding BCP and interatomic surface $S(\Omega,\Omega')$. The local properties of $\rho(\mathbf{r})$ at BCP have been demonstrated[19] to sum up very concisely the nature of the interaction occurring between the two linked atoms.

In this work we have investigated the values of $\rho(\mathbf{r})$ and of its Laplacian at the BCP's of the interactions involving the defective atoms. The electron density at BCP is expected to decrease with increasing bond length,[10] while the value of the Laplacian—the sum of the three eigenvalues λ_i $(\lambda_1\leqslant\lambda_2\leqslant\lambda_3)$ of the Hessian of $\rho(\mathbf{r})$ at the BCP—indicates whether the major contractions of the electron density in the interatomic surface are parallel or perpendicular to the AIL. The former $(\nabla^2\rho>0)$ are typical of the closed-shell interactions (ionic bonds, hydrogen bonds, van der Waals molecules), while the latter $(\nabla^2\rho<0)$ characterize the interactions (covalent and polar bonds) resulting from sharing of the electron density between atoms. The two negative curvatures at BCP define the bond ellipticity

$$\epsilon=\frac{\lambda_1}{\lambda_2}-1, \tag{4}$$

a measure of the extent to which the electron density is preferentially accumulated in a given plane at BCP.[20] Similarly one may define[21] a local ellipticity at each point of the AIL and the resulting trend of values shows how the electron density distribution deviates from cylindrical symmetry along the AIL.

In addition to supplying an analysis of the characteristics of atomic interactions, the Laplacian field allows one to recover also the chemical model of localized bonded and non-

TABLE I. Relative energies (units eV) along the BD evolution reaction coordinate. $\Delta E_{\mathrm{HF}}^{(a)}$ and $\Delta E_{\mathrm{HF}}^{(b)}$ data refer to set I and set II cluster, respectively.

$AA'B$	s	ΔE_{TBMD}	$\Delta E_{\mathrm{HF}}^{(a)}$	$\Delta E_{\mathrm{HF}}^{(b)}$
43°	0.00	0.00	0.00	0.00
49°	0.09	+0.25	+0.70	+0.16
65°	0.33	+1.24	+1.32	+2.05
91°	0.73	-1.78	-2.28	-2.42
109°	1.00	-3.51	-3.26	-3.57

bonded pairs and to characterize local concentrations ($\nabla^2\rho<0$) and depletions ($\nabla^2\rho>0$) of the electronic distribution.[19,22] The Laplacian field of an isolated atom reflects the quantum shell structure by exhibiting a corresponding number of alternating shells of charge concentration and charge depletion, beginning with a region of charge concentration at the nucleus. Upon bonding, local maxima and minima are formed in the valence shell charge concentration (VSCC) of a bonded atom and their number and properties depend on the linked atoms. Changes in the chemical environment of an atom (number, type, and geometrical arrangement of its neighbors) are mirrored in changes of number, magnitude, and location of its Laplacian local maxima in the atomic VSCC. These Laplacian maxima are referred to as *bonded* or *nonbonded* maxima according to whether they are located close to or far off AIL's.

C. Computations

A double-zeta basis set consisting of 13 atomic orbitals (AO's) ($4s$ and $9p$), resulting from 3-3-2-1G contractions, and 2 AO's ($2s$), resulting from 2-1G contractions, were used for Si and H, respectively. For Si the first contraction refers to s functions, while the remaining ones concern shells containing s and p functions sharing the exponents. This basis is referred to as 3-21G.[23] For the set II clusters the effect of polarization functions was investigated by supplementing the 3-21G basis with a single set of five d-type Gaussians on each Si atom (3-21G* basis set).[23]

The cluster electronic structures were obtained with the GAUSSIAN-94 (Ref. 24) program and the resulting wave functions were used as input for the AIMPAC (Ref. 25) package. The latter performs the topological analysis of the $\rho(\mathbf{r})$ and $\nabla^2\rho(\mathbf{r})$ scalar fields, and evaluates QTAM atomic properties.

III. RESULTS AND DISCUSSION

Table I reports the energy changes ΔE, with respect to $s=0$ along the BD evolution path. The RHF calculations on both cluster sets confirm that the BD complex rearranges to the nondefective system through a significant energy barrier. The set I RHF estimate (1.32 eV) is only 6% greater than the TBMD estimate (1.24 eV). When geometry relaxation is allowed in the RHF calculations (set II), the barrier is further raised to 2.05 eV. Table II lists the BCP properties for the bond interactions in the BD complex along the annihilation path. Also reported are the properties at Si–Si BCP in bulk silicon, which closely resemble those of the A-A' BCP at $s=1.00$ (cluster simulation of the nondefective system). Thus the innermost part of the nondefective cluster represents correctly the bulk and as a consequence the adopted clusters should adequately mimic the BD annihilation process. The QTAM predicts that all the Si atoms remain tetracoordinated along the process (Fig. 2), though the properties of the bond interactions change dramatically (Fig. 3). The BD annihilation requires the breaking of A-B (A'-B') and the formation of A-B' (A'-B) bonds, whereas the A-C type bonds are retained along the whole reaction path. In the BD complex

TABLE II. Si-Si BCP properties in bulk, in set I and set II (values in parentheses) clusters. Bond lengths are expressed in Å, ρ and $\nabla^2\rho$ in a.u.

Bond	Length (Å)	ρ	$\nabla^2\rho$	ϵ
$s=0$ (BD complex)				
A-A'	2.27 (2.21)	0.081 (0.090)	-0.104 (-0.133)	0.04 (0.03)
A-B	2.46 (2.45)	0.064 (0.066)	-0.056 (-0.065)	0.01 (0.01)
A-C	2.39 (2.39)	0.070 (0.071)	-0.072 (-0.079)	0.02 (0.01)
$s=0.09$				
A-A'	2.27	0.084	-0.112	0.05
A-B	2.62	0.053	-0.033	0.02
A-C	2.36	0.072	-0.079	0.02
$s=0.33$				
A-A'	2.27 (2.17)	0.084 (0.095)	-0.114 (-0.151)	0.12 (0.14)
A-B	3.01 (2.97)	0.030 (0.028)	+0.013 (+0.031)	0.41 (2.91)
A-C	2.33 (2.36)	0.074 (0.072)	-0.071 (-0.064)	0.12 (0.05)
$s=0.73$				
A-A'	2.27	0.081	-0.104	0.03
A-B'	2.69	0.049	-0.028	0.01
A-C	2.33	0.075	-0.090	0.01
$s=1$ (nondefective system)				
A-A'	2.36 (2.35)	0.073 (0.073)	-0.083 (-0.084)	0.00 (0.00)
bulk	2.36	0.074	-0.087	0.00

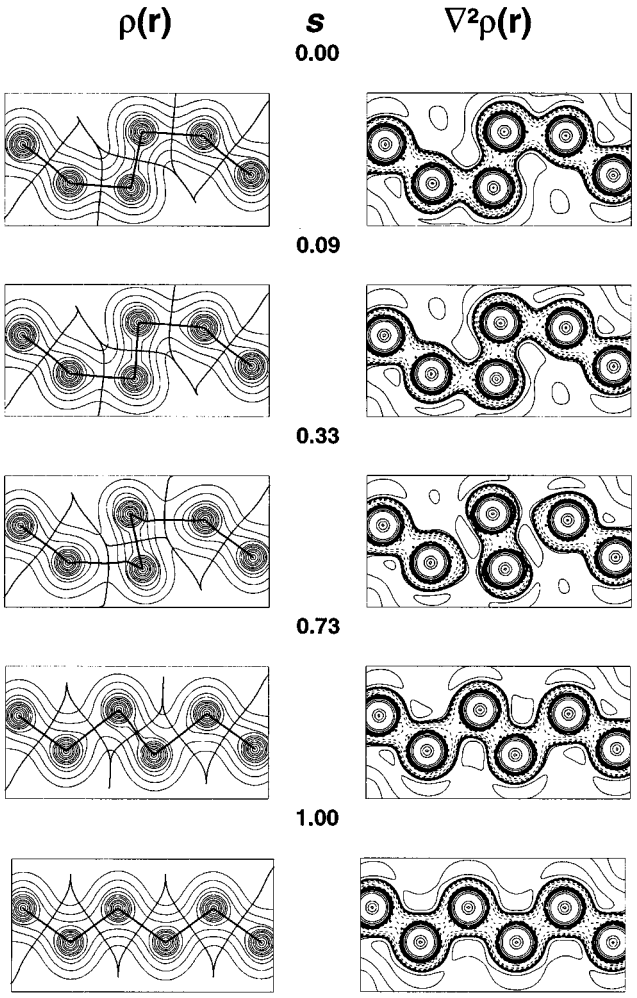

FIG. 3. Contour plots ($AA'BB'$ plane) of the electron density ρ (left) and its Laplacian $\nabla^2\rho$ (right) for the BD complex along its annihilation path. Atomic interaction lines and boundaries are superimposed on the electron density plots. The valence shell charge concentration $-\nabla^2\rho$ maxima are denoted by dots.

($s=0$) the A-A' distance is shortened (2.27 Å) with respect to the bulk (2.36 Å), while the A-B distance (2.46 Å) shows the opposite behavior. The A-C distance (2.39 Å) is quite similar to the bulk value and remains nearly constant along the reaction path s. The BCP properties of the BD complex indicate that all the bonds remain covalent as in the perfect lattice, while the observed changes in the values of ρ and $\nabla^2\rho$ agree with the reported internuclear distances—the density and the absolute value of the Laplacian decreasing (increasing) with increasing (decreasing) bond distance. The low ellipticity values show that all the bonds in the BD complex nearly retain the cylindrical symmetry.

At $s=0.33$ the Si-Si bonds are quite different in nature with respect to either the BD complex and the nondefective system. The geometrical relaxation in the TBMD simulation dramatically increases the A-B and only slightly decrease the A-C distance. The A-B and A-B' distances turn out to be nearly equal (3.01 and 3.08 Å, respectively) but only the A-B chemical interaction appears to be formed according to QTAM. However this interaction differs completely from the usual Si-Si bond, since the electron density at BCP lowers to

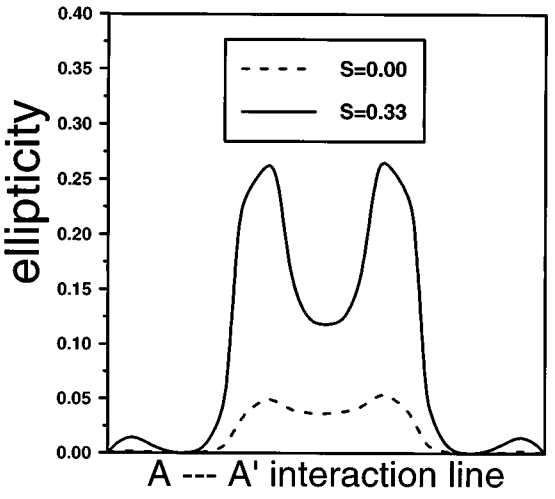

FIG. 4. Values of the ellipticity along the A-A' bond.

about 2/5 of the bulk value and the Laplacian is positive, thus denoting a marked shift towards a closed-shell-type interaction. At this step the A atoms appear to be only formally tetracoordinated, since they exhibit three covalent (and strong) bonds that lie nearly on a plane and a fourth weak closed-shell interaction out of this plane. The hybridization of A atoms is therefore closer to sp^2 rather than sp^3, a result confirmed below by the Laplacian topology. The A-A' and A-C bonds exhibit a significative increase of their ellipticity values, while maintaining covalent character and the other BCP properties similar to those at $s=0$. By analyzing the values of the curvatures and the direction of the associated eigenvectors, it turns out that the electron charge is (i) removed from the $AA'B$ plane along the AA' bond, and (ii) accumulated in planes perpendicular to the ACC' plane, along AC bonds. This mechanism, which is due to the formation of the A-B closed-shell interaction with the accompanying (concomitant) removal of charge from the internuclear region, is at variance with the usual[10] accumulation of charge in the π-bond direction. Figure 4 shows the trend of the ellipticity values along A-A' for the BD complex and for the $s=0.33$ configuration. The departure from the ideal tetrahedral coordination induces in both cases a removal of charge from the $AA'B$ plane with two maxima (and corresponding ellipticity maxima) associated with the two geometrically distorted A-B (A'-B') bonds. The larger is the distortion and the consequent closed-shell nature of the A-B bond ($s=0.33$), the higher are the maxima ($\epsilon=0.26$) associated to the charge removal.

Finally, at $s=0.73$ the A-B bond is broken and a new A-B' bond is formed, thus reconstructing the Si-Si network as in the bulk. The bond ellipticities decrease and approach zero, a value eventually reached at $s=1.00$. The new bond formed is far from being covalent in nature (the ratio of parallel to perpendicular curvature being three times that of the regular Si-Si bond), though the Laplacian at BCP is already negative.

Table II also shows the effect of full geometry relaxation (set II clusters) on the BCP properties along the reaction coordinate. The picture obtained with the larger and constrained clusters (set I) is qualitatively confirmed. First also

TABLE III. Value of $-\nabla^2\rho$ (a.u.) at the VSCC *bonded* and *nonbonded* maxima (see Fig. 5) of Si in set I clusters and in the bulk.

CP	$s=0$	$s=0.09$	$s=0.33$	$s=0.73$	$s=1$
Atom *A*					
1	0.118	0.126	0.132	0.118	0.100
2	0.093	0.099	0.126	0.112	0.098
3	0.073	0.050			
3*				0.041	0.097
Atom *B*					
4	0.081	0.069	0.078	0.073	0.098
Bulk					0.106

in this case the nondefective system mimics adequately the bulk. Second the RHF geometry relaxation shortens the *A*-*A*′ distance with respect to the TBMD prediction for the BD complex, but this distance does not notably change from $s=0$ to $s=0.73$. Finally the trend on BCP properties agrees with that found for set I. In particular, at $s=0.33$, the ellipticity increases are confirmed and the *A*-*B* bond is predicted to be even weaker than in set I (the density decreasing and the Laplacian increasing at BCP), in spite of a slightly shorter internuclear distance.

The changes in the number and magnitude of *bonded* (BM) and *nonbonded* (NBM) maxima of atoms *A* and *B* along the annihilation process are detailed in Table III. In the bulk each silicon atom exhibits four equivalent BM's, tetrahedrally arranged along the four Si-Si bonds (Fig. 5). The electron density rearrangement due to the formation of the BD complex, reduces the local symmetry around atoms *A* and *B* and removes the degeneracy in $-\nabla^2\rho$ values (Fig. 5 and Table III). The *B* atom retains four $-\nabla^2\rho$ maxima along the whole reaction path, thus preserving the $-\nabla^2\rho$ charge concentration pointing towards *A*-*A*′ even at large Si-Si distances. On the other hand, moving from the BD complex along the annihilation path, atom *A* undergoes a substantial decrease of the concentration labeled as 3 and pointing towards *B*, until this concentration disappears at $s=0.33$ where *A* exhibits only three maxima. These latter maxima and the *A* nucleus are nearly coplanar and their $-\nabla^2\rho$ values have significantly increased with respect to the bulk. The sp^2 picture for atom *A* at this stage of the annihilation process is confirmed. At the next step ($s=0.73$) the *A* atom exhibits again four maxima, but the concentration labeled as 3* in Table III and characterized by a very low $-\nabla^2\rho$ value, is

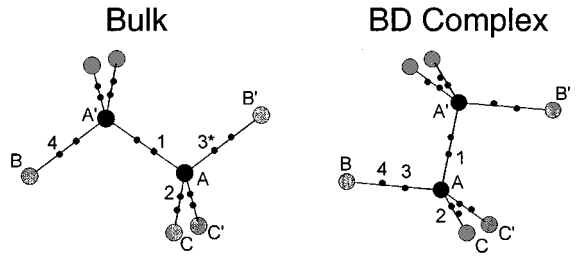

FIG. 5. Numbering and location of $-\nabla^2\rho$ bonded maxima in the BD complex and in the bulk.

TABLE IV. Si atomic basins properties in bulk and in set I clusters, along the *s* coordinate. All quantities are in a.u. Only the magnitude of dipole moments is reported. The parallel component of dipole moment is defined as follows: (i) for atom *A* $\mu_{||}$ is the projection of μ along vector *A*-*A*′; (ii) for atom *B*, $\mu_{||}$ is the projection along the vector *B*-*A**, where *A** denotes the regular lattice site; (iii) for atom *C* $\mu_{||}$ is the projection along vector *C*-*A*.

s	$N(\Omega)$	$V002(\Omega)$	μ	$\mu_{\|\|}$
Atom *A*				
0.00	13.720	126.3	0.64	0.63
0.09	13.702	128.3	0.79	0.79
0.33	13.962	141.8	1.30	1.27
0.73	13.853	138.8	0.81	0.80
1.00	13.996	139.5	0.05	0.02
Atom *B*				
0.00	14.011	155.7	0.13	-0.13
0.09	14.029	158.6	0.29	-0.29
0.33	14.135	167.3	0.89	-0.89
0.73	14.026	155.1	0.57	-0.56
1.00	13.988	145.5	0.13	-0.11
Atom *C*				
0.00	13.851	165.9	0.22	0.07
0.09	13.810	163.4	0.24	0.18
0.33	13.641	156.4	0.67	0.67
0.73	13.745	157.1	0.26	0.23
1.00	13.834	161.0	0.11	-0.01
Bulk atom	14.000	136.7	0.00	0.00

now pointing towards *B*′. Finally at $s=1$ the four concentrations of *A* are nearly equivalent and close to the bulk value, so confirming that the nondefective cluster adequately mimics the bulk.

Complementary information about the annihilation process is provided by the changes in the atomic properties along *s* as listed in Table IV for the set I clusters. The corresponding properties for the set II clusters follow the same trends and are not discussed for the sake of being concise. The first important observation is that the sum of the electron populations of the defective atoms $(2A+2B+4C)$ remains nearly constant and smaller by about 0.4–0.6 electrons with respect to the nondefective system. The table also shows that such charge depletion involves only the atoms of type *A* in the BD complex, while by proceeding along *s*, *C* atoms also become involved. The population of *C* reaches a minimum at $s=0.33$ in correspondence to a local maximum population for the *A* atom induced by the formation of an sp^2-sp^3 bond between *A* and *C*. On the other hand, the *B* atom is always more populated than in the bulk and its population raises up to 14.14 electrons at $s=0.33$. By considering their volume per electron, as provided by the $V002/N(\Omega)$ ratio, the atoms *A* and *B* are, respectively, more charge compressed and more charge depleted than in the nondefective system.

As what concerns the validity of our cluster simulation, one may note that in the nondefective system the population deficit of the ''defective atoms'' $(2A+2B)$ linked to silicon atoms only, amount to 0.032 electron charges. This tiny deficit is one order of magnitude smaller than the observed increase of the electron transfer from the defective atoms

$(2A+2B+4C)$ to the surroundings, found at each step of the annihilation path with respect to the nondefective system. On the basis of this observation, we feel confident that the significant leakage of an electron experienced by the defective atoms along the annihilation path is physically sound and not just the result of some spurious effect due to the cluster model.

The atomic dipole moment magnitudes are finally reported in the Table IV. Due to symmetry, the atomic dipole μ equals zero in bulk Si, while in the defective clusters, noticeable dipoles arise as a consequence of the lattice distortion induced by the formation and annihilation of the BD complex. The changes of the atomic dipoles along s are dominated by changes in their parallel component $\mu_{||}$. This latter is defined as the projection of μ along the A-A' (C-A) vector for atom $A(C)$ and as the projection of μ along the vector B-A^* for atom B (A^* denoting the regular lattice site). Within this definition, a positive (negative) value for $\mu_{||}$ indicates that the atomic centroid of negative charge moves outwards (inwards) the cluster inversion center. So in the BD complex atoms A and C are polarized outwards, while atoms B concentrate charge toward the defective system. Such a mechanism reaches a maximum at $s=0.33$ where the displacements of centroids from nuclear positions are as large as 0.025–0.050 Å. The atomic dipole magnitudes in the nondefective system, though different from zero, are about one order of magnitude lower than at $s=0.33$.

IV. CONCLUSIONS

Our *ab-initio* RHF calculations on both constrained and relaxed silicon clusters confirm the existence of a barrier for the annhilation of the BD complex found at the TBMD level. The RHF estimate of such a barrier and of the relative stability of the complex is in good agreement with finite-temperature TBMD simulations.

Our electron-density analysis indicates that in the BD complex about 0.5 electrons are subtracted from the defective atoms (i.e., from the $2A+2B+4C$ set of atoms of Fig. 5) and transferred to the surroundings. This charge leakage persists over the BD annihilation path. What is mostly changing along s is the relative contribution of the defective atoms. In the BD complex charge is removed *only* from A atoms, while at $s=0.73$ the charge leakage is evenly distributed among A and C atoms. At the barrier top the four C atoms are largely deprived of charge (-0.772 electrons), while the charge accumulation of the two B atoms is strongly enhanced ($+0.294$ electrons), thereby maximizing the charge transfer within the defective atoms. The reported charge rearrangments parallel the energy changes along s: the more unbalanced is the charge removal from defective atoms, the higher is the energy destabilization of the corresponding atomic environment. This observation rationalizes the existence of a barrier for BD annihilation and the smallest energy destabilization occurring at $s=0.73$, in spite of the observed largest ($+0.634$ electrons) leakage of electrons to the surroundings at this reaction step. The reach of the barrier top also involves a change of atoms A hybridization from sp^3 to sp^2, as evidenced from the calculated vanishing of their bonded maxima pointing towards B atoms and the concomitant increase in magnitude of their remaining bonded concentrations. Inspection of the bond characteristics at $s=0.33$ shows that only weak, closed-shell-like interactions occur between atoms A and B at the barrier top. This confirms the results of the $\nabla^2\rho$ topological analysis and the only formal tetracoordination of A atoms at this nuclear configuration.

In conclusion, the present study of the BD complex and its annihilation path demonstrates that QTAM may enhance our understanding of the defect electronic structure and of the mechanisms accompanying and governing its evolution. A ''chemical'' description of the migration path is obtained using a theoretical tool firmly rooted in quantum mechanics. The combination of TBMD simulations of defect formation, first-principles calculations of their electronic structure, and the topological analysis of the associated electron densities are likely a promising tool for the study of defect properties in bulk materials.

ACKNOWLEDGMENTS

L.C. acknowledges computational support by INFM under initiative ''Progetto di Supercalcolo'' (project ''Computer Simulations of Radiation Effects in Silicon''). C.G. acknowledges support by the Human Capital and Mobility program of the European Community under Contract No. CHRX-CT93-0155.

[1] M. Tang, L. Colombo, J. Zhu, and T. Diaz De La Rubia, Phys. Rev. B **55**, 14 279 (1997).

[2] U. Gösele and T. Y. Tan, *Diffusion in Solids, Unsolved Problems* (Trans Tech, Zurich, 1992), p. 189.

[3] I. Kwon, R. Biswas, C. Z. Wang, K. M. Ho, and C. M. Soukoulis, Phys. Rev. B **49**, 7242 (1994).

[4] F. Cargnoni, L. Colombo, and C. Gatti, Nucl. Instrum. Methods Phys. Res. B **127–128**, 235 (1997).

[5] A. Fortunelli, A. DeSalvo, O. Salvetti, and E. Albertazzi, in *Cluster Models for Surface and Bulk Phenomena*, edited by G. Pacchioni, P. S. Bagus, F. Parmigiani, Vol. 283 of NATO ASI Series B (Plenum, New York, 1992), p. 595.

[6] C. C. J. Roothaan, Rev. Mod. Phys. **23**, 69 (1951); G. G. Hall, Proc. R. Soc. London Ser. A **205**, 541 (1951).

[7] The validity of our assumption has been tested by performing restricted open Hartree-Fock (ROHF) calculations along the annihilation path on the set II clusters. The corresponding ROHF energies predict the triplet to be always significantly unstable (>2 eV) with respect to the singlet state, save at $s=0.33$. At this point the singlet is still the most stable state, but the two electron configurations are nearly degenerate as their energy difference amounts to 0.28 eV at the singlet optimized geometry (vertical transition) and lowers to 0.01 eV when geometry relaxation is allowed (adiabatic transition). At $s=0.33$, or in its close neighborhood, an intersystem crossing (from singlet to triplet) might actually occur. However, on the basis of the large energy differences found at all other points along the annihilation path, including the starting (BD complex) and final (the nondefective

system) ones, the study of the corresponding energy curve for the singlet state only is thoroughly justified.

[8] C. Pisani, R. Dovesi, and R. Orlando, Int. J. Quantum Chem. **42**, 5 (1992).

[9] C. Möller and M. S. Plesser, Phys. Rev. **46**, 618 (1934).

[10] R. F. W. Bader, *Atoms in Molecules. A Quantum Theory*, International Series of Monographs on Chemistry, Vol. 22 (Oxford University Press, Oxford, 1990).

[11] R. F. W. Bader, Phys. Rev. B **49**, 13 348 (1994).

[12] C. Gatti, V. R. Saunders, and C. Roetti, J. Chem. Phys. **101**, 10 686 (1994).

[13] M. E. Eberhart, M. M. Donovan, and R. A. Outlaw, Phys. Rev. B **46**, 12 744 (1992).

[14] M. E. Eberhart, D. P. Clougherty, and J. M. MacLaren, J. Mater. Res. **8**, 438 (1993).

[15] J. Schwinger, Phys. Rev. **82**, 914 (1951).

[16] R. F. W. Bader, M. T. Carroll, J. R. Cheeseman, and C. Chang, J. Am. Chem. Soc. **109**, 7968 (1987).

[17] R. F. W. Bader and H. J. T. Preston, Theor. Chim. Acta **17**, 384 (1970).

[18] R. J. Mulliken, J. Chem. Phys. **23**, 1833 (1955); **23**, 2343 (1955).

[19] R. F. W. Bader and H. Essen, J. Chem. Phys. **80**, 1943 (1984).

[20] R. F. W. Bader, T. S. Slee, D. Cremer, and E. Kraka, J. Am. Chem. Soc. **105**, 5061 (1983).

[21] J. R. Cheeseman, M. T. Carroll, and R. F. W. Bader, Chem. Phys. Lett. **141**, 450 (1988).

[22] R. W. F. Bader, P. J. MacDougall, and C. D. H. Lau, J. Am. Chem. Soc. **106**, 1594 (1984).

[23] W. J. Hehre, L. Radom, P. V. R. Schleyer, and J. A. People, *Ab initio Molecular Orbital Theory* (Wiley, New York, 1986).

[24] GAUSSIAN 94 (Revision A.1), M. J. Frisch, G. W. Trucks, H. B. Schlegel, P. M. W. Gill, B. G. Johnson, M. A. Robb, J. R. Cheeseman, T. A. Keith, G. A. Petersson, J. A. Montgomery, K. Ragavachari, M. A. Al–Laham, V. G. Zagrewski, J. V. Ortiz, J. B. Foresman, J. Cioslowski, B. B. Stefanov, A. Nanayakkara, M. Challacombe, C. Y. Peng, P. Y. Ayala, W. Chen, M. W. Wong, J. L. Andres, E. S. Replogle, R. Gomperts, R. L. Martin, D. J. Fox, J. S. Binkley, D. J. Defrees, J. Baker, J. P. Stewart, M. Head-Gordon, C. Gonzalez, and J. A. Pople, Gaussian Inc., Pittsburgh PA, 1995.

[25] AIMPAC, McMaster University, Ontario, Canada, 1992.